Transmission Electron Microscopy

Part VIII: Conventional TEM of Perfect and Defective Crystalline Specimen

Christoph T. Koch
Max Planck Institut für Metallforschung

Literature: Marc de Graef, “Introduction to Conventional Transmission Electron Microscopy”, Cambridge University Press, Cambridge (2003)

Website about defects in crystals:
http://www.tf.uni-kiel.de/matwis/amat/def_en/index.html
http://www.gpm2.inpg.fr/axes/plast/MicroPlast/ddd/TEM/index.php

Conventional TEM Image Contrast

Dynamical image contrast in conventional (not atomic-resolution) images may be affected by:

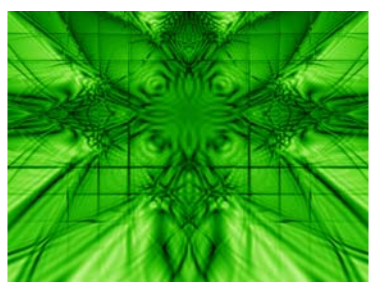

- Variations in specimen thickness (i.e. thickness fringes)
- Variations in specimen orientation (e.g. bend contours)
- Strain fields around
  - Planar defects
  - Dislocations
  - Point defects
- Super-imposed crystalline structures (Moiré fringes)

Dynamical Theory: Multiple Elastic Scattering

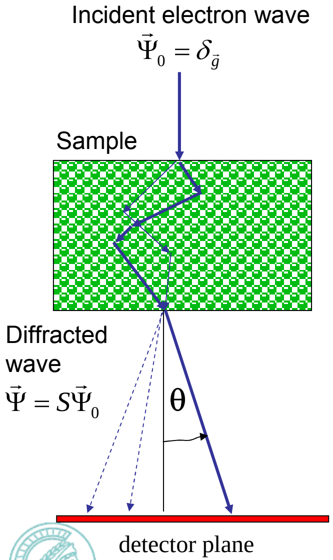

Scattering Matrix

Diagonal matrix with (variable) experimental parameters

$$S = \exp(iT[\tilde{\boldsymbol{A}} + \boldsymbol{G}(k_t)])$$

Beam tilt

Matrix with material properties (atoms and their positions)

$$T = \pi\gamma\lambda t$$

GaAs (110) potential

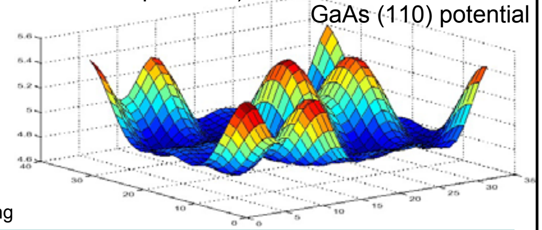

Structure Factor Matrix A = Ã+G(k_t)

$$\tilde{A}_{n,m} = U_{\vec{g}_n - \vec{g}_m}$$

$$G_{n,n} = \xi_n = -(|\vec{g}_n|^2 + \vec{g}_n \cdot \vec{k}_t)/\gamma$$

Example: symmetric 5-beam case with refelctions $\vec{g}_1$, $\vec{g}_2$, $\vec{g}_3 = 0$, $-\vec{g}_1$, and $-\vec{g}_2$:

$$\tilde{A} = \begin{pmatrix} 0 & U_{-\vec{g}_1+\vec{g}_2} & U_{\vec{g}_2} & U_{\vec{g}_1+\vec{g}_2} & U_{2\vec{g}_2} \\ U_{\vec{g}_1-\vec{g}_2} & 0 & U_{\vec{g}_1} & U_{2\vec{g}_1} & U_{\vec{g}_1+\vec{g}_2} \\ U_{-\vec{g}_2} & U_{-\vec{g}_1} & 0 & U_{\vec{g}_1} & U_{\vec{g}_2} \\ U_{-\vec{g}_1-\vec{g}_2} & U_{-2\vec{g}_1} & U_{-\vec{g}_1} & 0 & U_{-\vec{g}_1+\vec{g}_2} \\ U_{-2\vec{g}_2} & U_{-\vec{g}_1-\vec{g}_2} & U_{-\vec{g}_2} & U_{\vec{g}_1-\vec{g}_2} & 0 \end{pmatrix}$$

$$G(\vec{k}_t) = \begin{pmatrix} -|\vec{g}_2|^2 - \vec{g}_2 \cdot \vec{k}_t & 0 & 0 & 0 & 0 \\ 0 & -|\vec{g}_1|^2 - \vec{g}_1 \cdot \vec{k}_t & 0 & 0 & 0 \\ 0 & 0 & 0 & 0 & 0 \\ 0 & 0 & 0 & -|\vec{g}_1|^2 + \vec{g}_1 \cdot \vec{k}_t & 0 \\ 0 & 0 & 0 & 0 & -|\vec{g}_2|^2 + \vec{g}_2 \cdot \vec{k}_t \end{pmatrix}$$

A fast electron in a periodic potential V(**r**)

(Bloch wave method: Hans Bethe, 1928)

The relativistic Schrödinger equation (Klein Gordon equation) for a fast electron:

$$\nabla^2\Psi(\vec{r}) + \frac{2m|e|}{\hbar^2}\left[E + V(\vec{r})\right]\Psi(\vec{r}) = 0$$

Expanding Ψ(r) using **Bloch's theorem**, the Laplace operation on the wave function can be written in reciprocal space as:

$$\nabla^2\Psi = -4\pi^2 \sum_j \Psi_j \sum_{\vec{g}} C_{\vec{g}}^{(j)} (\vec{k}^{(j)} + \vec{g})^2 \exp(2\pi i(\vec{k}^{(j)} + \vec{g}) \cdot \vec{r})$$

A somewhat lengthy derivation shows that the $C_g^{(j)}$-coefficients must also be the elements of the eigenvector matrix of the so called **structure factor matrix** and $\left(k_z^{(j)} - K\right)$ its eigenvalues, but also, that given these, the reciprocal-space wave function behind the crystal (z=t) can be obtained by that in front of it (z=0) according to:

$$\vec{\tilde{\Psi}}(\vec{k}_t, t) = \underbrace{C\left[\exp(2\pi i k_z^{(j)} t)\right]_D C^{-1}}_{\boxed{\text{Scattering matrix } S(k_t,\lambda,t)}} \vec{\tilde{\Psi}}(\vec{k}_t, 0)$$

2-Beam Geometry

Only the beam $\mathbf{g}_3$ intersects the Ewald sphere (in addition to the (0,0,0)-beam, of course) and is therefore strongly excited.

Different 2-beam conditions can be set up.

The diffraction condition in which mainly reflections in a single line are excited (i.e. a 1-dimensional diffraction pattern) is called **systematic row** case.

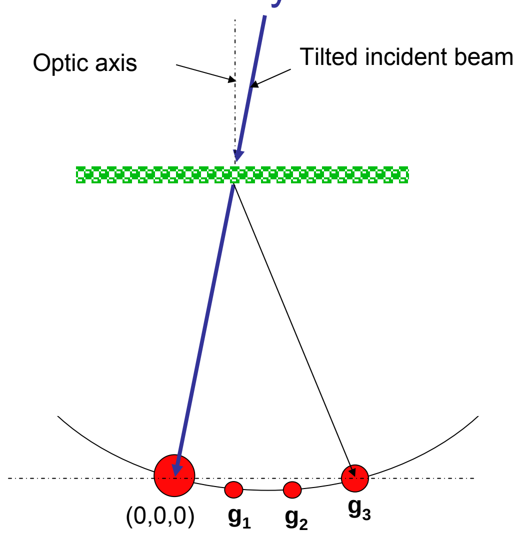

2-Beam Dynamical Diffraction

A crystal is said to be oriented in a 2-beam condition, if the Ewald sphere only intersects a single reflection **g** aside from the central beam.
The structure factor matrix may then be reduced to a simple 2 x 2 matrix:

$$A = \begin{pmatrix} 0 & U_{-\vec{g}} \\ U_{\vec{g}} & 0 \end{pmatrix} + \begin{pmatrix} 0 & \\ & -|\vec{g}|^2 - \vec{g} \cdot \vec{k}_t \end{pmatrix}$$

The scattering matrix S can be found analytically in this case, leading to an intensity in the diffracted beam of:

$$I_g = \lambda^2 \left|U_g\right|^2 \frac{\sin^2\left(\pi t \sqrt{s_g^2 + \lambda^2 \left|U_g\right|^2}\right)}{s_g^2 + \lambda^2 \left|U_g\right|^2}$$

Excitation error in 2-beam condition: $s_g = -\dfrac{g \cdot k_t}{2}$
(This defines kt=0 in the exact 2-beam condion)

Pendelösung Plots

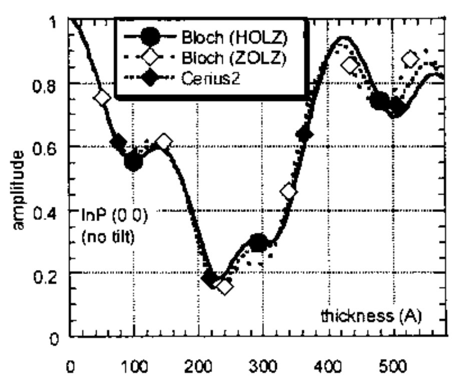

Plot of the (dynamical) intensity of the central beam of a diffraction pattern of InP (100) as a function of specimen thickness.
Computed by 2 different methods:

- Bloch wave method (with and without HOLZ line contributions
- Multislice (Cerius2-software) [see STEM lecture]

In the 2-beam condition the intensity in the diffracted beam is just 1-I(g=0).

Single Reflection Imaging

A small objective aperture may be used to select the transmitted beam or a single reflection of a crystalline specimen in the back-focal plane of the objective lens. Such images may reveal properties of the sample not visible otherwise.

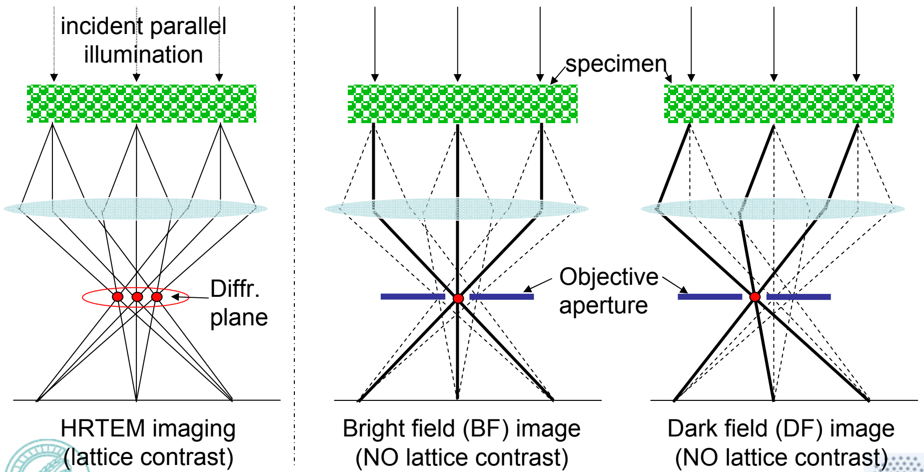

Contrast in Single Reflection Images

Single reflection images reveal the amount of intensity scattered into a single reflection. BF/DF images are therefore sensitive to local thickness and lattice orientation (e.g. strain).

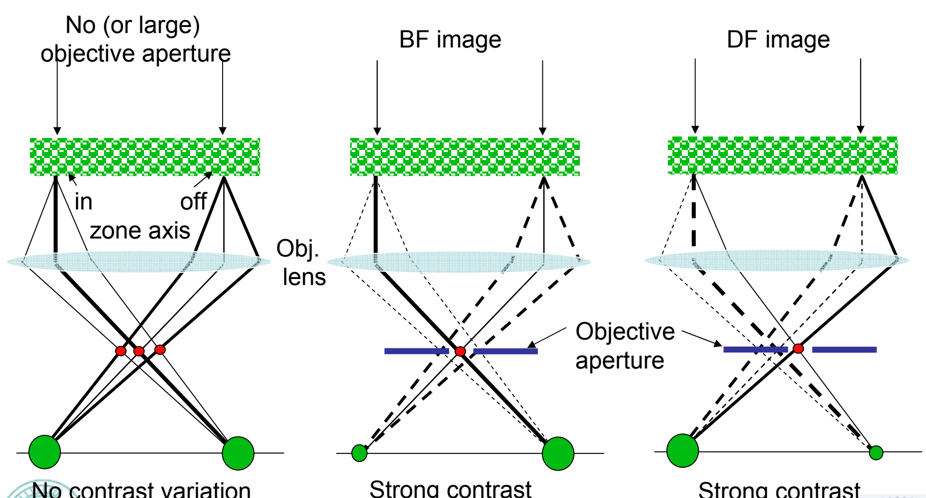

Thickness Fringes

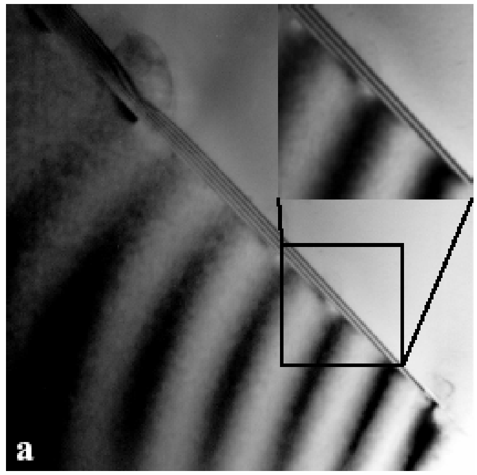

Thickness fringes in a BF image of a grain that is in, or close to a zone axis and shows therefore strong dynamical effects.

Image: book by M. de Graef

Thickness Fringes @ Surface steps

The high sensitivity of the dynamical diffraction pattern to the specimen thickness may reveal single atom layer surface steps.

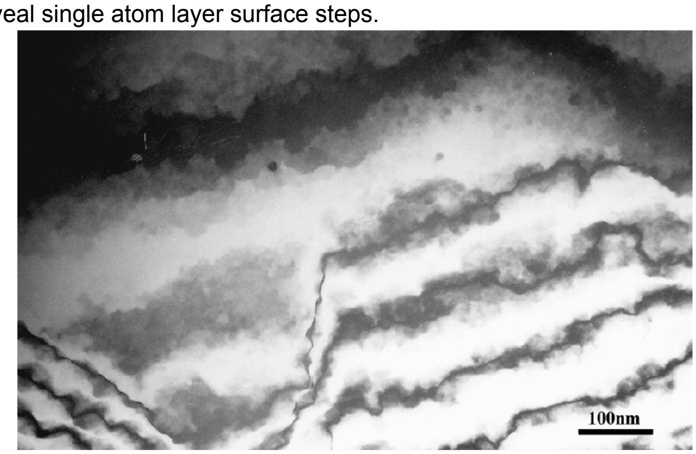

SiC (111)
(Objective aperture included central beam and Si (422)/3 forbidden reflections)

CBED Pattern = 2D Rocking Curves

Diffracted intensity in reflection **g** for a given transverse component of the incident wave vector $\mathbf{k}_t$ away from the exact zone axis:

$$I_g(\mathbf{k}_t)=|S_{g,0}(\mathbf{k}_t)|^2 = |\exp(iT[\tilde{\mathbf{A}} + \mathbf{G}(\mathbf{k}_t)])|^2$$

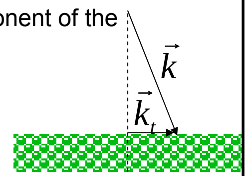

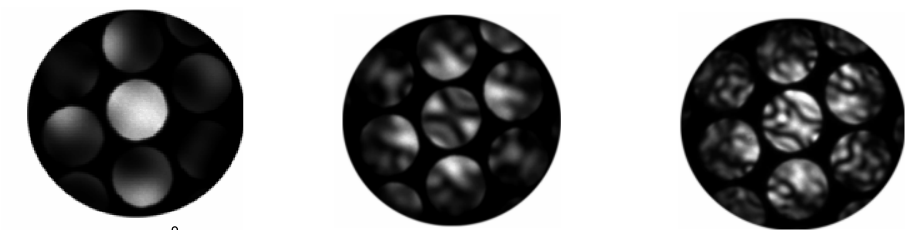

t=300Å t=850Å t=1580Å

Experimental (zero-loss filtered) CBED pattern of Si (110). The specimen thickness has been determined by matching the pattern with simulated ones. => Small changes in specimen-beam alignment have dramatic effects on the diffracted intensity in a given reflection, especially in thick samples!

Bright-Field Image of a Curved Sample

The diffraction of a parallel electron beam in a bent (curved) specimen may be treated as an electron beam with spatially varying angle of incidence on a straight sample.
Since the diffracted intensities depend on the angle of incidence, a rocking curve will be super-imposed on the image of the sample. The contrast of this rocking curve (**bend contours**) depends on the **objective aperture** being used.

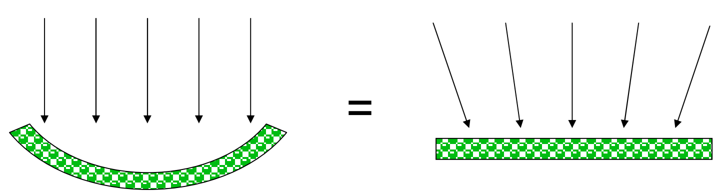

Bend Contours

A bright-field image of a curved specimen shows the intensity of the central beam of the (dynamical) diffraction pattern at each specimen position. These contrast variations indicate the local diffracting conditions and thus the **local crystal orientation**.

Bent contour contrast is strongly related to the contrast observed in **convergent beam electron diffraction**, where the orientation of the incident beam changes instead of the specimen orientation.

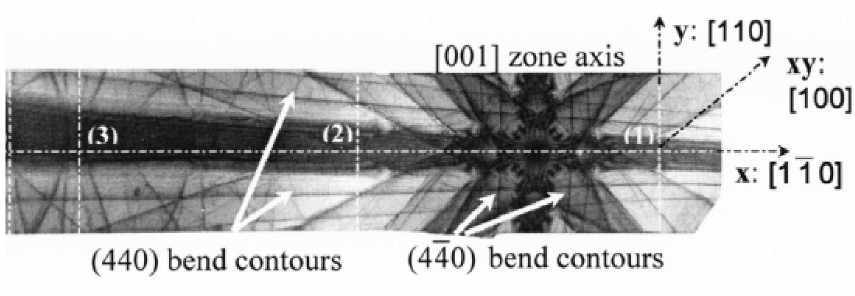

Image: Cabié et al., Appl. Phys. Lett. 86 (2005) 191901

Point- and Line Defects in a Crystal Structure

Defects in crystal structures produce strain fields around them, thus locally changing the orientation of the lattice with respect to the incident electron beam.

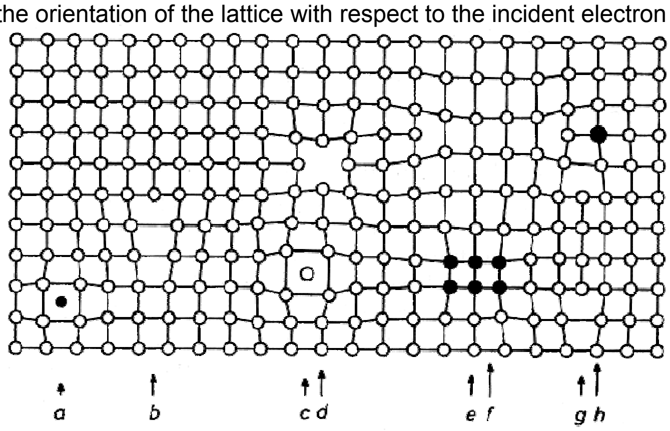

a) Interstitial impurity atom, b) Edge dislocation, c) Self interstitial atom, d) Vacancy, e) Precipitate of impurity atoms, f) Vacancy type dislocation loop, g) Interstitial type dislocation loop, h) Substitutional impurity atom

Dislocations

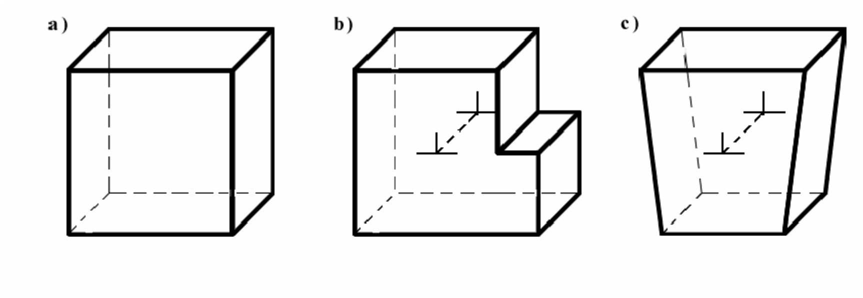

Operations producing pure edge dislocations a) perfect crystal cube b) shear: the horizontal lattice constant of the top part of the crystal due to shear stress differs from the one on the bottom. Misfit dislocations account for the displacement on the atomic level. c) dilatation: edge dislocations moving through the perfect crystal structure account for material shift in ductile processes.

60° Edge Dislocation in Si

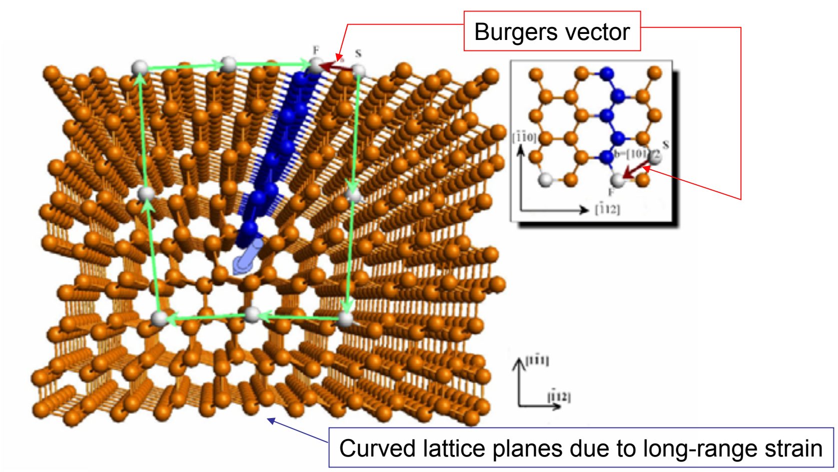

Burgers circuit in diamond cubic structure containing a dislocation running int
the plane of the paper as indicated by the round (blue) arrow. The length and direction o
the Burgers vector is the difference between the points S and F. The inset shows a portio
of the top plane, showing that the Burgers vector $b = \frac{a}{2}[10\bar{1}]$ is not in the plane of th
paper, but at a 60° angle with respect to the dislocation line.

Dissociated Dislocation

In fcc crystals a 60° edge dislocation may dissociate into 2 partial dislocations with a stacking fault between them.

$$\begin{array}{ccc} \vec{b}_{60^\circ} & \longrightarrow & \vec{b}_{30^\circ} + \vec{b}_{90^\circ} \\ \frac{a}{2}[10\bar{1}] & \longrightarrow & \frac{a}{6}[21\bar{1}] + \frac{a}{6}[1\bar{1}\bar{2}] \end{array}$$

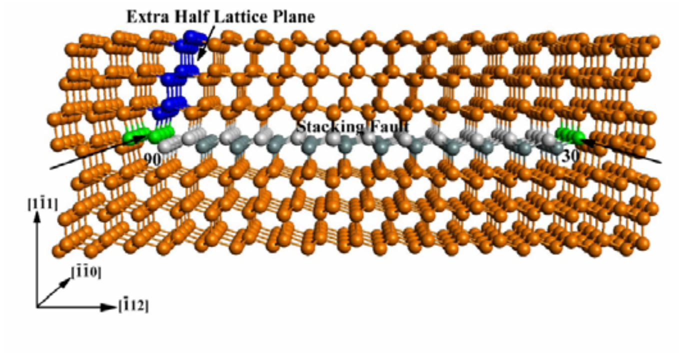

Dissociated 60° glide-set dislocation. A stacking fault (SF) ribbon (plane of gray and white atoms) is bound by the two partials. The cores (green) of the 30° and the 90° partial are reconstructed. The extra half plane at the 90° partial is indicated by the blue atoms.

Dislocations in BF images

BF image of dislocations in Si(111). The dissociation of dislocations into partials can be seen very clearly. The very weak contrast features concentric around the small area of vacuum at the top of the image are Pendellösung fringes.

Screw Dislocations

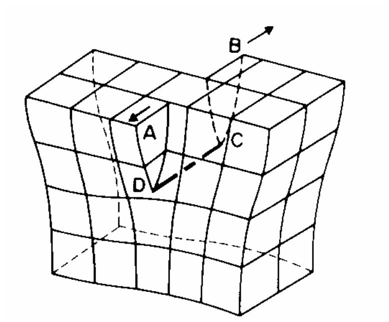

Model of a screw dislocation

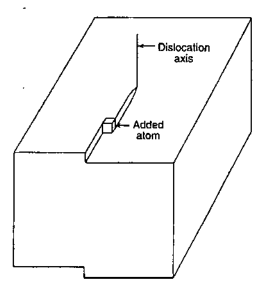

Spiral crystal growth around the core of a screw dislocation

Edge Dislocations at Low-Angle Grain Boundaries

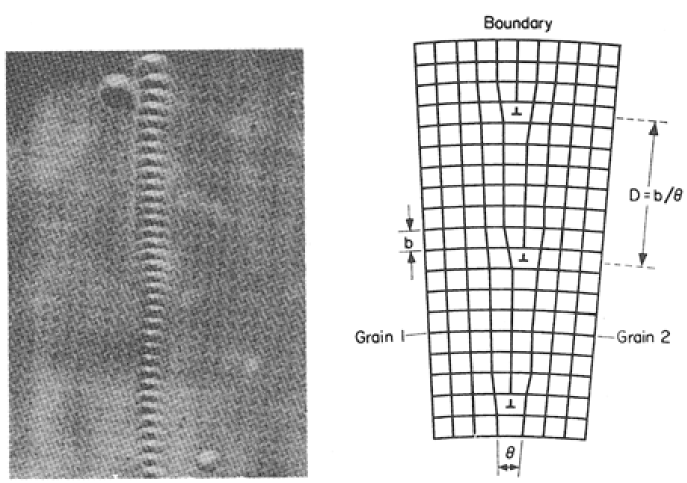

(a) (b)

Imaging Dislocations

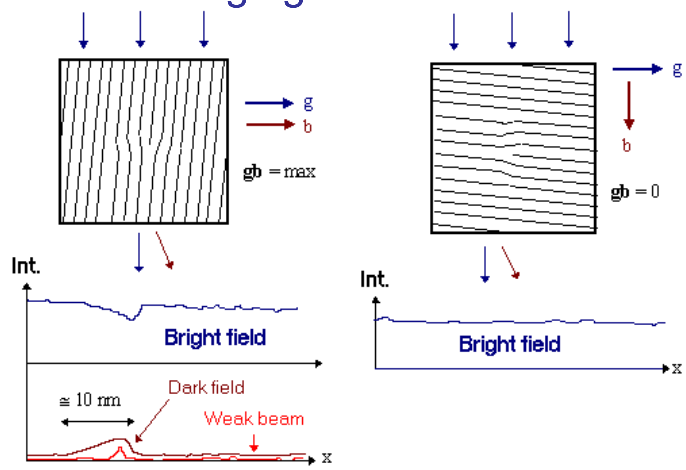

A Burgers vector of **b** of a dislocation produces a local shift in lattice constant in the direction **b**. If a 2-beam condition for reflection **g** is set up, contrast of dislocations whose Burgers vector is parallel to **g** is maximized.

Weak Beam Imaging

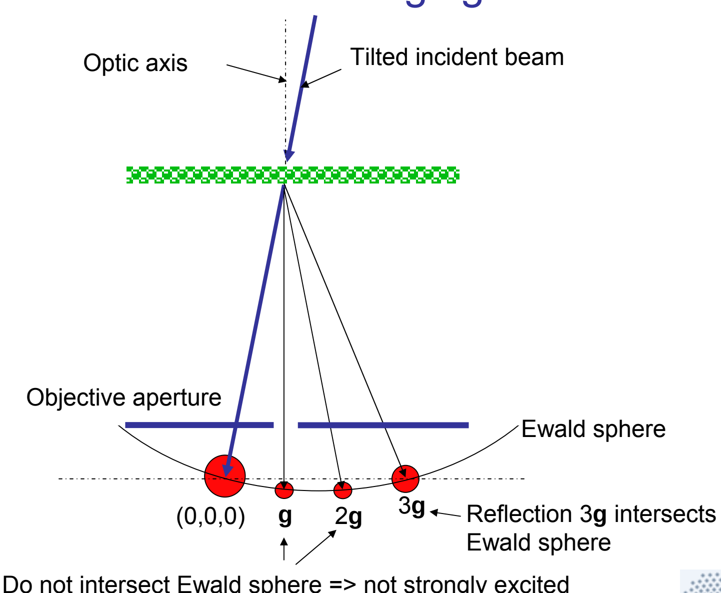

Weak-Beam Imaging: Select what you want to see

Shown are two weak-beam images of the same area of a dislocation network with threefold symmetry in a small angle grain boundary in Silicon. Difference between the images: diffracting condition.

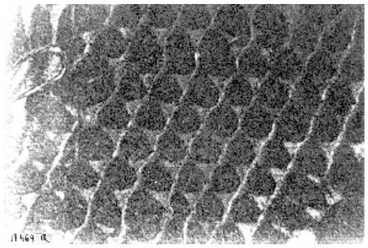

Only one set of dislocations and one kind of stacking fault is visible

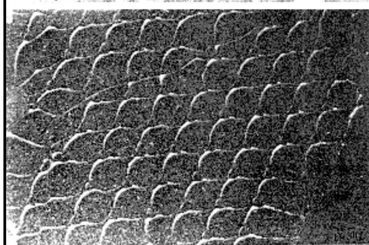

Two sets of dislocations are visible; the stacking faults are invisible.

Weak beam images are very low in intensity (they require several minutes of illumination), but they have quite high resolution.

Real-Time Observation of Dislocation Motion

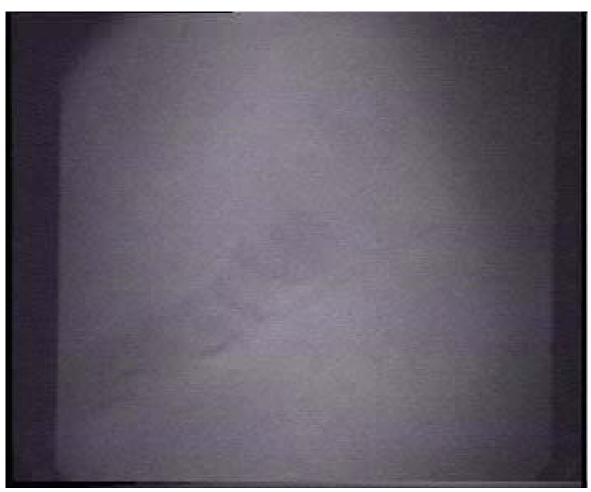

BF Movie of cross slip events in Ge at high temperature

http://www.gpm2.inpg.fr/axes/plast/MicroPlast/ddd/TEM/mechanisms/propagation.php

Dislocation Cross Slip

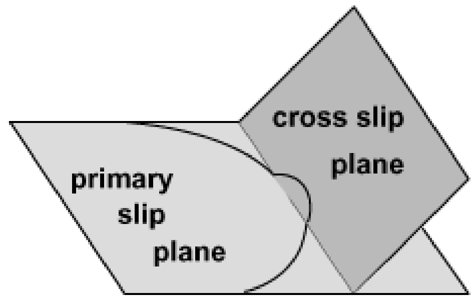

The screw part of a dislocation loop may deviate in a cross slip plane. The dislocation Burgers vector is along the intersection of the primary and the cross slip planes.

Annihilation of Dislocations

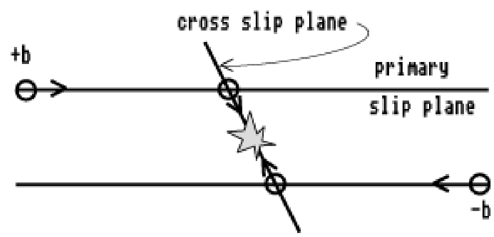

Two dislocations with opposite Burgers vector move in parallel planes.

Owing to their mutual attraction, they may deviate on their cross slip plane and annihilate.

Real-time Observation of Dislocation Interaction

BF Movie of pile-up and cross slip in Ge at high temperature.

http://www.gpm2.inpg.fr/axes/plast/MicroPlast/ddd/TEM/mechanisms/propagation.php

Dislocation Interaction

Dislocations with opposite Burgers vectors glide in opposite directions on parallel planes. Owing to their attractive interactions, they slow down as they fly over each other.

http://www.gpm2.inpg.fr/axes/plast/MicroPlast/ddd/TEM/mechanisms/propagation.php

Imaging Dislocation Networks in 3D: Weak Beam Tomography

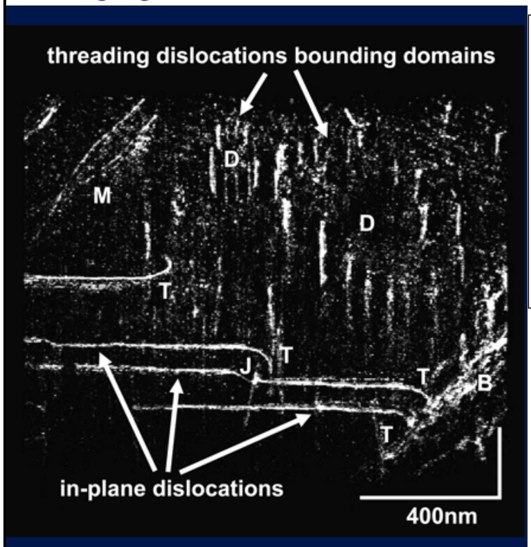

GaN film showing walls of threading dislocations surrounding domains (D), a dislocation bundle (B) associated with a crack, and threading dislocations that turn over at T to become in-plane dislocations and terminate at the specimen surface. Each turn over T occurs at a different height in the film, and one has interacted with a threading dislocation, causing a jog (J). Dislocations of mixed character (M) are also visible.

<u>α-GaN (wurtzite) grown on sapphire</u>
cracks due to partial delamination
=> dislocation networks.

J. S. Barnard, et al. *Science* **313** (2006) 319

Covering a larger range of beam tilt angle in CBED

A rocking curve across a large range of incident beam orientations can be obtained by recording (convergent beam) diffraction patterns at different beam tilts.

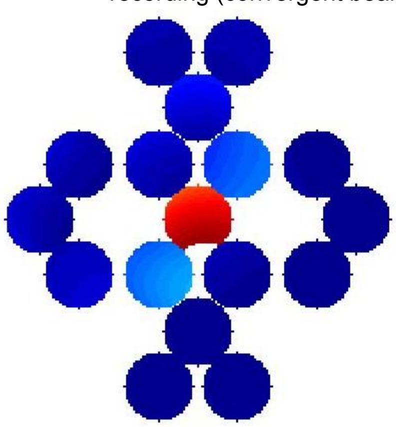

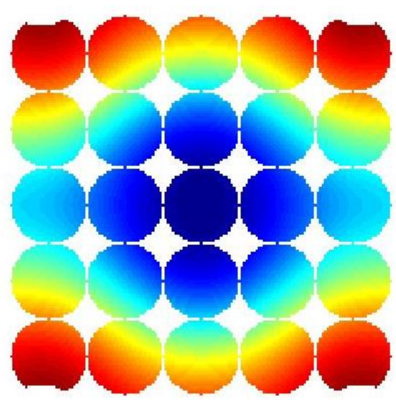

GaAs [011], t=35A

Large Angle Convergent Beam Electron Diffraction (LACBED)

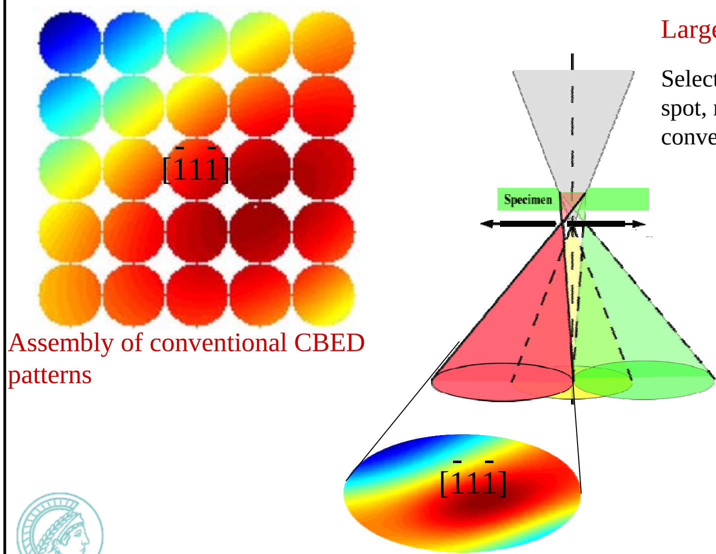

Large Angle (LA) CBED

Select a single diffraction spot, no overlap, despite large convergence angle

Intermediate Image Aperture Selects Diffraction Disc

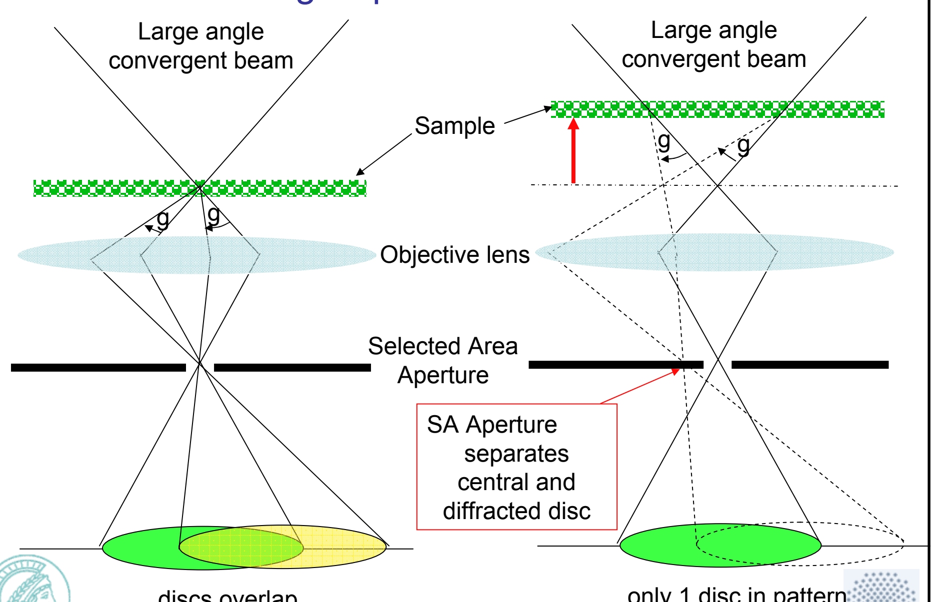

Investigation of Planar Defects using LACBED

Twins in $LaGaO_3$

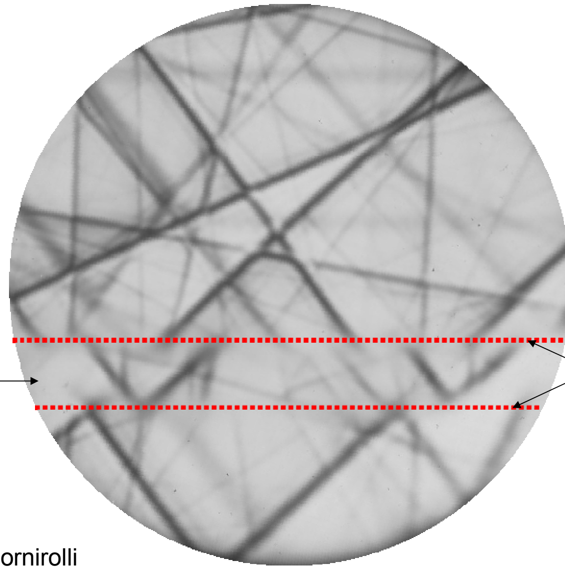

Image: J.P. Mornirolli

Investigation of Line Defects by LACBED

In LACBED, the 3-dimensional Burgers vector of a dislocation can be identified from a single pattern.
The intersection of a HOLZ line with the dislocation line splits up into **g**·**b**=n fringes (**b**=Burgers vector, **g**=reciprocal lattice vector of HOLZ line).
Each intersection therefore provides the projection of the Burgers vector onto this particular lattice plane, and the 3-dimensional Burgers vector can be reconstructed from all 3 intersections.

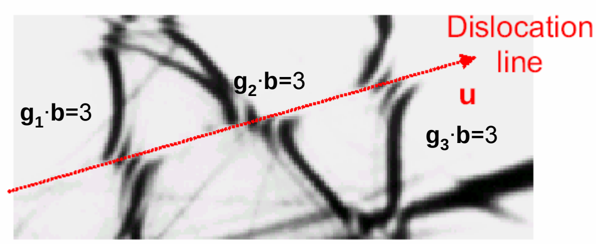

If the dislocation line intersects with only one HOLZ line, the sample (or illumination) can be shifted to make it intersect with another HOLZ line.

Moiré Imaging

The superposition of 2 lattices (either of different size or of equal size but rotated w.r.t. one another) produces fringes of the coincident site lattice (CSL).

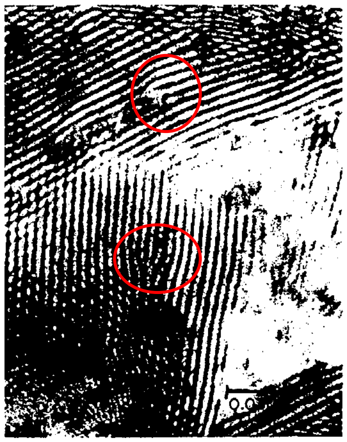

- Moire pattern from Pd layer deposited on to (111) Au film.
- The circles illustrate the location of the dislocations.
- $D_{1(022)Pd}$ = 0.137 nm and $D_{2(022)Au}$ = 0.144 giving a Moire magnification of ≈ 20.

Thickness Fringes @ Surface steps

The high sensitivity of the dynamical diffraction pattern to the specimen thickness may reveal single atom layer surface steps.

Image: F. Ross, IBM

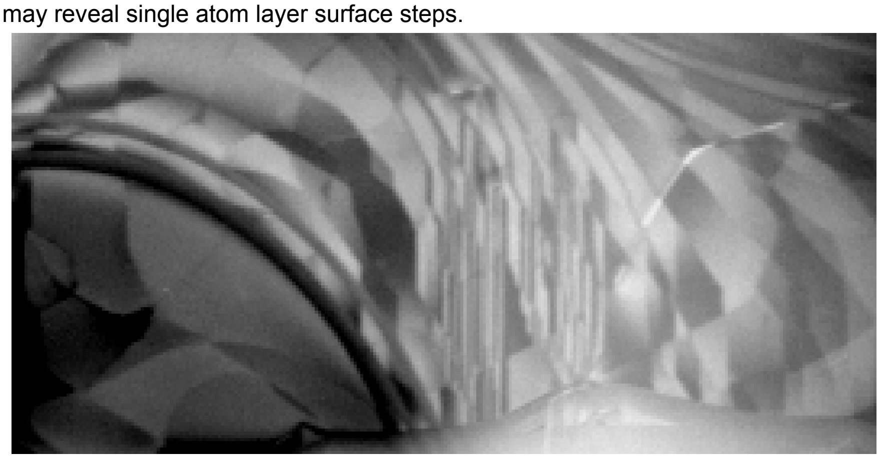

Si after High Temp. flashing in UHV-TEM
(Objective aperture included Si (422)/3 forbidden reflections)